Effect of heterogeneous risk perception on information diffusion, behavior change, and disease transmission

Yang Ye [1], Qingpeng Zhang [1,*], Zhongyuan Ruan [2], Zhidong Cao [3,4,5], Qi Xuan [2], and Daniel Dajun Zeng [3,4,5]

[1]*School of Data Science, City University of Hong Kong, Hong Kong SAR, China*
[2]*Institute of Cyberspace Security, Zhejiang University of Technology, Hangzhou, Zhejiang, China*
[3]*State Key Laboratory of Management and Control for Complex Systems, Institute of Automation,*
Chinese Academy of Sciences, Beijing, China
[4]*School of Artificial Intelligence, University of Chinese Academy of Sciences, Beijing, China*
[5]*Shenzhen Artificial Intelligence and Data Science Institute, Shenzhen, Guangdong, China*

Motivated by the importance of individual differences in risk perception and behavior change in people's responses to infectious disease outbreaks (particularly the ongoing COVID-19 pandemic), we propose a heterogeneous disease-behavior-information transmission model, in which people's risk of getting infected is influenced by information diffusion, behavior change, and disease transmission. We use both a mean-field approximation and Monte Carlo simulations to analyze the dynamics of the model. Information diffusion influences behavior change by allowing people to be aware of the disease and adopt self-protection and subsequently affects disease transmission by changing the actual infection rate. Results show that (a) awareness plays a central role in epidemic prevention, (b) a reasonable fraction of overreacting nodes are needed in epidemic prevention (c) the basic reproduction number R_0 has different effects on epidemic outbreak for cases with and without asymptomatic infection, and (d) social influence on behavior change can remarkably decrease the epidemic outbreak size. This research indicates that the media and opinion leaders should not understate the transmissibility and severity of diseases to ensure that people become aware of the disease and adopt self-protection to protect themselves and the whole population.

I. INTRODUCTION

People's responses to infectious diseases could greatly affect the transmission patterns of diseases, and information about the transmissibility and severity of the disease conveyed through the media and opinion leaders plays a central role in raising awareness and influencing people's decision-making on whether or not to adopt self-protection, i.e., taking recommended practices to reduce the risk of infection, such as wearing a mask and washing hands with sanitizer in the COVID-19 context [1–7]. Here opinion leaders refer to individuals whose opinions are widely accepted by other people [8,9].

Many studies [10–16] used mathematical models to investigate how disease awareness affects the outbreaks of diseases. Most approaches [17,18] explored this problem by modifying the parameters in standard epidemic models. Funk *et al.* [19] first incorporated the effect of awareness into classic epidemic models and found that the spread of awareness could substantially reduce the epidemic outbreak size. Gross *et al.* [20] studied epidemic dynamics on an adaptive network in which susceptible nodes avoid contact with infected nodes by rewiring their connections. Wu *et al.* [21] modeled the effect of three forms of awareness: global awareness, local

awareness, and contact awareness. They showed that only global awareness cannot decrease the likelihood of an epidemic outbreak. Chen [22] examined how the amount of information affects behavior change and showed that increasing the amount of information that people possess may lower the likelihood of disease eradication.

Multiplex (also named multilayer) networks [23,24] have been developed to model the dynamic interactions between the spread of information and infection. The spreading of information and infection is represented by multiple network layers. For example, Granell *et al.* [25] proposed the susceptible-infected-susceptible unaware-aware-unaware model that can capture the critical point of the disease outbreak determined by the topological structure of the virtual information diffusion network. It can be extended to many model variants, such as the multiple-information model [26] that incorporates more than one type of information; the local awareness controlled contagion spreading model [27], in which the awareness transition is further influenced by the extent of the awareness of all neighbors; and the susceptible-infected-recovered (SIR) unaware-aware model [28] that also considers the recovered state. In addition to information diffusion and disease transmission, the transmission of protective behavior has been simulated [29].

Recent studies examined the effect of the media on infectious disease epidemics [30–37]. Liu *et al.* [32] proposed a mechanism to illustrate the effect of the media by

_____
*qingpeng.zhang@cityu.edu.hk

incorporating the reported numbers of infectious and hospitalized individuals into classic epidemic models. Wang and Xiao [33] used a threshold model where the media can exhibit its effect only when the number of reports reaches a certain value. Dubey *et al.* [34] and Cramer *et al.* [35] discussed the optimal amount of information that not only can suppress the transmission of the disease but also prevents "media fatigue." Song and Xiao [36,37] further considered the delay of media effects on people's responses.

To summarize, existing studies indicate that the interplay between awareness and social network structure could greatly influence the transmission of infectious diseases. However, few studies have considered individual differences in people's responses to messages conveyed through the media and opinion leaders during epidemics. People's responses are influenced not only by the transmissibility and severity of the disease, but also by their personal risk perception [38–40]. Here risk perception refers to the subjective judgment about the risk of the disease. Similar to smart nodes in information diffusion [41,42], individuals who are more fearful of being infected actively engage in self-protection and information sharing. We label these people as overreacting as compared with underreacting people who have a relatively low risk perception. This classification can also be applied to the novel coronavirus (COVID-19) epidemic, in which a clear disparity in risk perception causes the diverse reactions of individuals regarding control measures [43–46]. Lessons from the COVID-19 outbreak in many countries imply that people responding properly to the disease is more important than simple awareness.

Motivated by the importance of individual differences in risk perception and behavior change in people's responses to infectious disease outbreaks (particularly the ongoing COVID-19 pandemic), we propose a heterogeneous disease-behavior-information transmission model, which consists of information diffusion, behavior change, and disease transmission. This model aims to describe how different types of nodes (overreacting versus underreacting) influence the prevalence of protective behavior and the epidemic outbreak. The contribution of this study is threefold. First, this is a quantitative study that examines the incorporation of risk perception and disease-behavior-information transmission on a multilayer network. Second, we consider individual differences in the responses to disease-related information originating from variations in the distribution of risk perception among people. Third, we study analytically and numerically the effect of such differences on the epidemic.

The rest of the paper is organized as follows. First, we describe the model details in Sec. II. Then we adopt the mean-field method [47] to formulate the problem mathematically in Sec. III. Next we perform extensive experiments with Poisson degree distribution-based networks and explore the effects of different parameters on the epidemic outbreak in Sec. IV. We conclude the paper with a summary and discussion of future work in Sec. V.

II. MODEL

We propose a three-layer network model, namely, the heterogeneous disease-behavior-information (HDBI) trans-
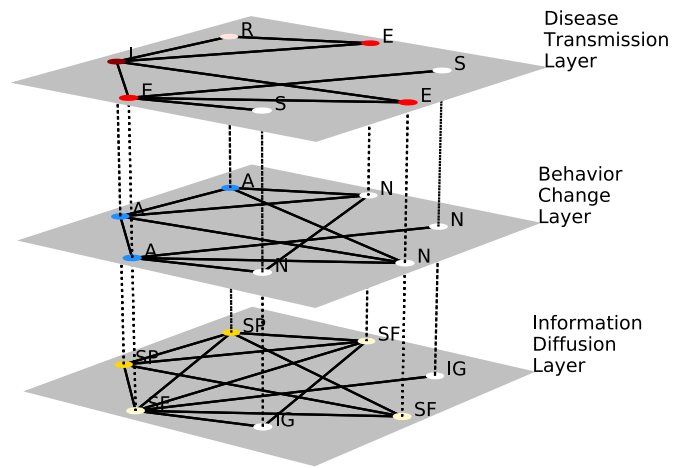

FIG. 1. Structure of the three-layer network framework. The bottom, middle, and top layers represent information diffusion, behavior change, and disease transmission, respectively.

mission model, to incorporate information diffusion, behavior change, and disease transmission. Here nodes may become aware of the risk of getting infected and then change their behavior by adopting self-protection, which will further affect the disease transmission. We first introduce the details as shown in Fig. 1. All layers in the model contain the same set of nodes.

On the bottom layer, namely, the information diffusion layer, edges represent the social contacts through which nodes can share the disease-related information. The sources of the information are the media and opinion leaders. Nodes are divided into three classes on this layer: ignorants, spreaders, and stiflers, denoted by *IG*, *SP*, and *SF*, respectively. Ignorants are those who are unaware of the disease-related information and can become spreaders (with a probability α) or stiflers (with a probability $1 - \alpha$) if at least one neighbor is a spreader. Spreaders and stiflers are those who are aware of the disease. We assume that the states of spreaders and stiflers do not change for simplification. Once a spreader, the node will keep spreading the information to all its neighbors in each period. Stiflers, on the other hand, do not further spread the information. We present the scheme mentioned above in Fig. 2(c).

Each piece of information has an alarming level y, which represents the transmissibility and severity of the disease conveyed through the media and opinion leaders. Each node on the network has a personal risk perception, a constant parameter x_i for node i. By comparing the values of y and x_i, we classify nodes into two sets: $\{i \mid y \geqslant x_i\}$, overreacting, and $\{i \mid y < x_i\}$, underreacting. Overreacting nodes have a higher probability to spread the information as

$$\alpha = \begin{cases} \alpha_o, & y \geqslant x_i \\ \alpha_u, & y < x_i, \end{cases} \quad (1)$$

where $0 \leqslant \alpha_u < \alpha_o \leqslant 1$.

On the middle layer, namely, the behavior change layer, edges represent the social contacts through which a node can observe other nodes' states of behavior change. Nodes on this layer have two states: adopted self-protection A and not
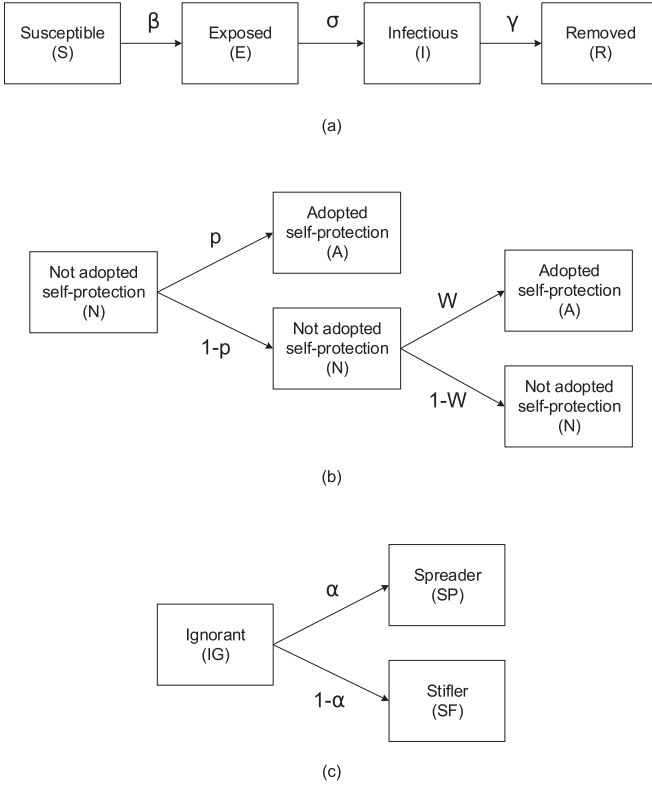
FIG. 2. Illustration of the transitions between states on (a) the disease transmission layer, (b) the behavior change layer, and (c) the information diffusion layer. The ignorants are unaware of the disease and the spreaders and stiflers have become aware of the disease. Here α and p correspond, respectively, to α_o and p_o for overreacting nodes and α_u and p_u for underreacting nodes.

adopted self-protection N. Ignorants on the information diffusion layer are always in the N state on the behavior change layer because they are unaware of the risk. Spreaders and stiflers have a tendency p to change the behavior by adopting self-protection and overreacting nodes have higher behavior change tendency than underreacting nodes as

$$p = \begin{cases} p_o, & y \geqslant x_i \\ p_u, & y < x_i, \end{cases} \tag{2}$$

where $0 \leqslant p_u < p_o \leqslant 1$.

The probability of a node to change behavior is dependent on not only p, but also the behavior of its neighbors. The behavior change result can be determined in two steps. First, we use the tendency p to determine if the node changes the behavior independent of the social influence. If the node does not change the behavior, then the model further checks its neighbors' states. If more than half of the nodes in its ego network (the node and all its neighbors) have changed behavior, then the node will be influenced to change as well. Letting k denote the degree of a node and z denote the number of its neighbors who have already changed behavior, we use φ to summarize all neighbors' states as

$$\varphi = \begin{cases} 1, & z > k - z + 1 \\ 0, & z \leqslant k - z + 1. \end{cases} \tag{3}$$

The smallest integer value of z satisfying $\varphi = 1$ is $\lceil \frac{k+2}{2} \rceil$; thus the overall behavior change probability is

$$\mathcal{P} = p + (1 - p)W, \tag{4}$$

where $W = P(\varphi = 1) = P(z \geqslant \lceil \frac{k+2}{2} \rceil)$. We present the scheme mentioned above in Fig. 2(b).

The top layer, the disease transmission layer, is modeled by the generalized susceptible-exposed-infectious-recovered (SEIR) model. Edges represent the physical contacts through which diseases may be transmitted. The susceptible, exposed, infectious, and recovered nodes are denoted by S, E, I, and R, respectively. A susceptible node can be infected by either an infectious node with an infection rate β_I or an exposed node with an infection rate β_E. In the classic SEIR model, exposed nodes are infected but do not develop symptoms or become infectious. Here we allow the transmission from exposed nodes to model the widely reported asymptomatically infected cases in the COVID-19 pandemic and other similar disease outbreaks [48–50]. If we set $\beta_E = 0$, then this layer is identical to the classic SEIR model. For simplicity and consistency with previous work [51,52], the HDBI model ignores the transition from asymptomatically infected to recovered. However, the model is flexible in incorporating various asymptomatic scenarios.

The infection rate β (including β_I and β_E) is a constant value only related to the disease. The actual infection rate could vary because of different self-protection outcomes. Considering an edge connecting two nodes, we use $n \in \{0, 1, 2\}$ to denote the number of nodes who have adopted self-protection. The actual transition rate is $\eta^n \beta$, where η is the ineffectiveness of self-protection behavior. Here $\eta \in [0, 1]$; η is 0 if the self-protection behavior is fully protective and 1 if the self-protection behavior is entirely useless. An exposed node has a transition rate σ to become infectious, so the incubation period is $1/\sigma$. An infectious node has a transition rate γ to become recovered and immune to the same disease. All possible state transitions are shown in Fig. 2(a).

III. THEORETICAL ANALYSIS

We adopt the mean-field approximation approach to analyze the dynamics of the HDBI model. This technique assumes independence among the random variables and helps us study the complex stochastic model with a simpler model [47,53,54]. For simplicity, we consider a three-layer network with the same topological structure. We consider a network of N nodes with a Poisson degree distribution $P(k)$, where k denotes the degree of a node.

On the information diffusion layer, $\rho_{IG}(t)$, $\rho_{SP}(t)$, and $\rho_{SF}(t)$ denote the fraction of ignorants, spreaders, and stiflers at time t, respectively. Thus, $\rho_{IG}(t) + \rho_{SP}(t) + \rho_{SF}(t) = 1$. An ignorant remains unaware only if none of its neighbors are spreaders. Hence, the probability that an IG node with degree k not being informed by any neighbor is $[1 - \rho_{SP}(t)]^k$. Thus, the transition rate for a randomly selected IG node being informed by neighbors is

$$h(t) = 1 - \sum_{k=0}^{k_{\max}} P(k)[1 - \rho_{SP}(t)]^k, \tag{5}$$

where $k_{\max}$ denotes the maximum degree of the network.

Assuming a standard normal distribution of the risk perception x_i, we can calculate the fraction of overreacting nodes by evaluating the corresponding cumulative distribution function at the alarming level y, denoted by a. Thus, those who are aware of the disease will become spreaders with a probability $a\alpha_o + (1 - a)\alpha_u$ or become stiflers with a probability $a(1 - \alpha_o) + (1 - a)(1 - \alpha_u)$.

On the behavior change layer, letting $\rho_A(t)$ denote the fraction of nodes having adopted self-protection at time t, then the probability for a node with degree k to choose to protect itself because of the social influence from neighbors is

$$
W_k = \begin{cases} 0 & k = 0, 1 \\ \sum_{b=\lceil (k+2)/2 \rceil}^{k} \binom{k}{b}[\rho_A(t)]^b[1 - \rho_A(t)]^{k-b} & \text{otherwise,} \end{cases}
$$

which is equal to the probability that at least $\lceil \frac{k+2}{2} \rceil$ neighbors have adopted self-protection; thus the probability of changing behavior due to the social influence from neighbors for a randomly selected node is $W = \sum_{k=0}^{k_{\max}} P(k)W_k$. Therefore, the probability of changing behavior is $p_o + (1 - p_o)W$ for overreacting nodes and $p_u + (1 - p_u)W$ for underreacting nodes [according to Eq. (4)]. In addition, ignorants will never adopt self-protection; thus the fraction of nodes who might adopt behavior change at time $t + 1$ is $\rho_{SP}(t + 1) + \rho_{SF}(t + 1)$. So we can get the fraction of nodes having adopted self-protection at time $t + 1$ as follows:

$$
\begin{aligned}
\rho_A(t + 1) = &[\rho_{SP}(t + 1) + \rho_{SF}(t + 1)]\{ap_o + (1 - a)p_u \\
&+ [a(1 - p_o) + (1 - a)(1 - p_u)]W\},
\end{aligned} \tag{6}
$$

Therefore,

$$
\rho_N(t + 1) = 1 - \rho_A(t + 1), \tag{7}
$$

which is the fraction of nodes having not adopted self-protection at time $t + 1$.

On the disease transmission layer, the fraction of nodes in one of the four health states at time t is denoted by $\rho_S(t)$, $\rho_E(t)$, $\rho_I(t)$, and $\rho_R(t)$; $\rho_S(t) + \rho_E(t) + \rho_I(t) + \rho_R(t) = 1$. For a single edge between a susceptible node and an infected one, the probability that both have adopted self-protection is $[\rho_A(t)]^2$ and the corresponding actual transition rate is $\eta^2\beta$. The probability that both nodes have not adopted self-protection is $[1 - \rho_A(t)]^2$ and the corresponding actual transition rate is $\eta^0\beta$. The probability that only one of them has adopted self-protection is $1 - [\rho_A(t)]^2 - [1 - \rho_A(t)]^2$ and the corresponding actual transition rate is $\eta^1\beta$. Thus, the actual infection rate $l(\beta)$ is

$$
\begin{aligned}
l(\beta) = &[\rho_A(t)]^2\eta^2\beta + [1 - \rho_A(t)]^2\eta^0\beta + \{1 - [\rho_A(t)]^2 \\
&- [1 - \rho_A(t)]^2\}\eta^1\beta = \beta[1 + (\eta - 1)\rho_A(t)]^2. \tag{8}
\end{aligned}
$$

For a node of state I, the infection propagates to its S neighbors with probability $l_I = l(\beta_I)$. For an exposed node who is asymptomatically infected, the corresponding probability $l_E = l(\beta_E)$. For a node of degree k with b_E neighbors in states E and b_I neighbors in state I, the probability of being infected is $q_{b_E,b_I} = 1 - (1 - l_E)^{b_E}(1 - l_I)^{b_I}$, where $(1 - l_E)^{b_E}(1 - l_I)^{b_I}$ is the probability that the node is not infected by any infected neighbors. Thus, the transition probability for
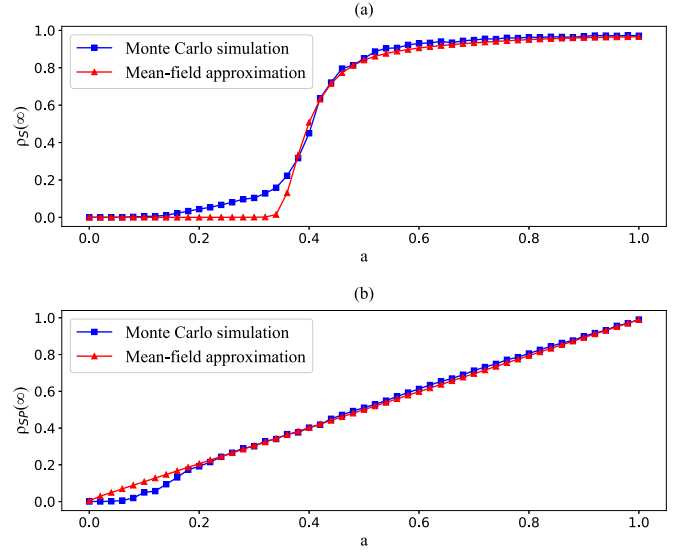

FIG. 3. (a) Comparison of the Monte Carlo simulation and the mean-field approximation results of the relationship between the fraction of susceptible nodes at the stationary state $\rho_S(\infty)$ and the fraction of overreacting nodes a and (b) the relationship between the fraction of spreaders at the stationary state $\rho_{SP}(\infty)$ and a. The parameters are $\beta_I = 0.5$, $\beta_E = 0$, $\sigma = 0.8$, $\gamma = 0.5$, $\eta = 0.1$, $\alpha_o = p_o = 0.99$, and $\alpha_u = p_u = 0.01$.

a susceptible node being infected at time t is

$$
c(t) = \sum_{k=0}^{k_{\max}} P(k) \sum_{b_E=0}^{k} \sum_{b_I=0}^{k-b_E} r_{k,b_E,b_I} q_{b_E,b_I}, \tag{9}
$$

where

$$
\begin{aligned}
r_{k,b_E,b_I} = &\binom{k}{b_E}\binom{k - b_E}{b_I}\{[\rho_E(t)]^{b_E}[\rho_I(t)]^{b_I} \\
&\times [1 - \rho_E(t) - \rho_I(t)]^{k-b_E-b_I}\} \tag{10}
\end{aligned}
$$

represents the probability of a node with degree k having b_E neighbors in state E and b_I neighbors in state I at time t. Then we can obtain the following equations to describe the dynamics on the disease transmission layer and the information diffusion layer in Fig. 1:

$$
\begin{aligned}
\rho_S(t + 1) - \rho_S(t) &= -c(t)\rho_S(t), \\
\rho_E(t + 1) - \rho_E(t) &= -\sigma\rho_E(t) + c(t)\rho_S(t), \\
\rho_I(t + 1) - \rho_I(t) &= -\gamma\rho_I(t) + \sigma\rho_E(t), \\
\rho_R(t + 1) - \rho_R(t) &= \gamma\rho_I(t), \\
\rho_{IG}(t + 1) - \rho_{IG}(t) &= -h(t)\rho_{IG}(t), \\
\rho_{SP}(t + 1) - \rho_{SP}(t) &= h(t)\rho_{IG}(t)[a\alpha_o + (1 - a)\alpha_u], \\
\rho_{SF}(t + 1) - \rho_{SF}(t) &= h(t)\rho_{IG}(t)[a(1 - \alpha_o) \\
&\quad + (1 - a)(1 - \alpha_u)]. \tag{11}
\end{aligned}
$$

The dynamics on the behavior change layer are described by Eqs. (6) and (7). Information diffusion influences the behavior change by determining the fraction of individuals who are being aware of the disease and adopting self-protection accordingly [from Eq. (6)]. Disease transmission is
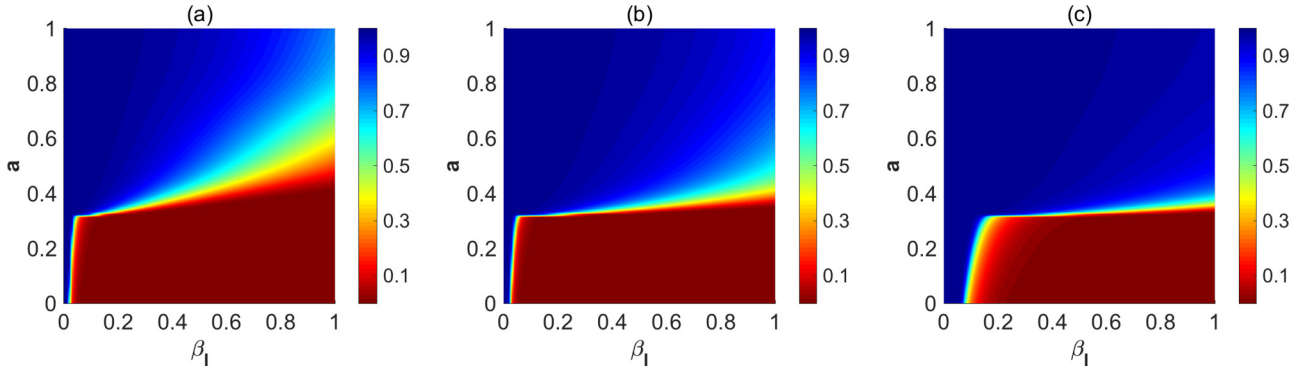
FIG. 4. Full a-β_I phase diagrams of the fraction of susceptible nodes at the stationary state $\rho_S(\infty)$ for different values of σ and γ without asymptomatically infected cases, where $\eta = 0.1$, $\alpha_o = p_o = 0.99$, and $\alpha_u = p_u = 0.01$. The values of σ and γ are set as follows: (a) $\sigma = 0.8$ and $\gamma = 0.2$, (b) $\sigma = 0.2$ and $\gamma = 0.2$, and (c) $\sigma = 0.2$ and $\gamma = 0.8$.

subsequently affected by changing the actual infection rate based on the outcome of behavior change [from Eq. (8)].

IV. RESULTS

We perform extensive Monte Carlo simulations to validate the mean-field approximation results obtained by Eqs. (11). For simplicity, we assume that $\alpha_o = p_o = 0.99$ and $\alpha_u = p_u = 0.01$, indicating an extremely high probability to inform others and to change behavior for overreacting nodes and a much lower probability for underreacting nodes.

We present the comparison between the Monte Carlo simulation and the mean-field approximation results in Fig. 3 for a three-layer network of 2000 nodes with a mean degree of 15. We adopt the synchronous updating method [55] in the Monte Carlo simulations to mimic the discrete-time transmission processes in our model. All nodes are selected to update their states simultaneously in each time step. The time step is set as 1. At the beginning of each simulation, we randomly select a node to be the initially infected node and another to be the first spreader. The updating process stops when there is no infected node in the network. Each point in Fig. 3 is obtained by averaging 50 Monte Carlo simulations. As illustrated in Fig. 3, we observe a high R^2 of 0.990 for Fig. 3(a) [the fraction of susceptible nodes at the stationary state $\rho_S(\infty)$], and 0.994 for Fig. 3(b) [the fraction of spreaders at the stationary state $\rho_{SP}(\infty)$]. This finding validates that Eqs. (11) can effectively

capture the dynamics of the model. Here the stationary state refers to the state at $t \to \infty$. Moreover, the fraction of overreacting nodes a has a linear effect on $\rho_{SP}(\infty)$ but a sigmoid effect on $\rho_S(\infty)$.

We examine the degree to which the overreacting nodes influence the disease dynamics under different situations. Analytical solutions for Eqs. (11) are difficult to obtain. Thus, full phase diagrams are used to illustrate the results. We adopt the same three-layer network mentioned in the aforementioned Monte Carlo simulations.

First, we focus on the diseases without asymptomatically infected cases (i.e., $\beta_E = 0$). The fraction of susceptible nodes at the stationary state $\rho_S(\infty)$ is shown in Fig. 4, concerning the infection rate β_I and the fraction of overreacting nodes a. When $\beta_E = 0$, the disease transmission layer is essentially an SEIR model. Given fixed values of a, the infection rate β_I has a reverse-sigmoid effect on $\rho_S(\infty)$, which is similar to the SIR and SEIR models [56,57]. Similar to Fig. 3, a has a sigmoid effect on $\rho_S(\infty)$ as shown in Fig. 4. We find that $\rho_S(\infty)$ generally has three phases: When a is small, $\rho_S(\infty)$ is close to 0, and when a is large, $\rho_S(\infty)$ is close to 1. A threshold triggers the rapid increase in $\rho_S(\infty)$. The exact value of the threshold cannot be analytically obtained. This indicates that by increasing the fraction of overreacting nodes through highlighting the transmissibility and severity of the disease, we can largely prevent the disease outbreak. As long as the fraction of overreacting nodes reaches the
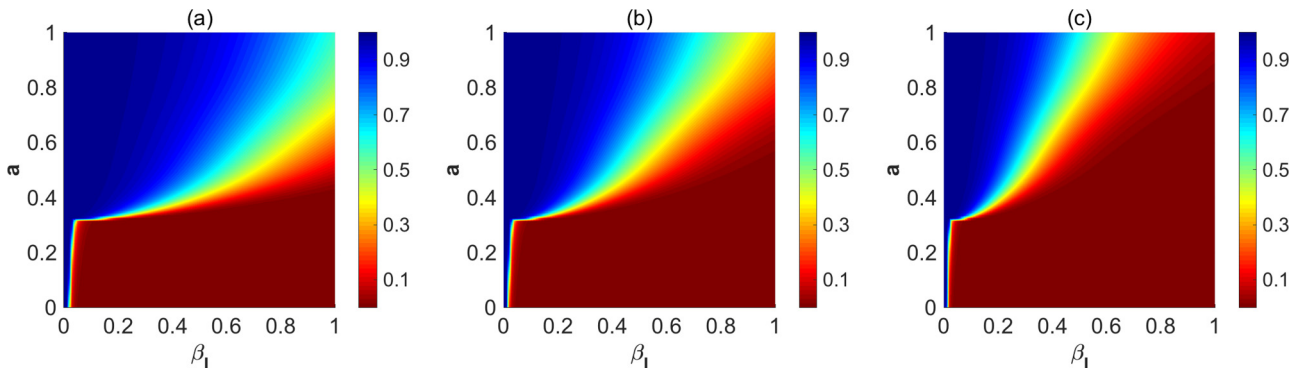

FIG. 5. Full a-β_I phase diagrams of the fraction of susceptible nodes at the stationary state $\rho_S(\infty)$ for different values of β_E, where $\eta = 0.1$, $\alpha_o = p_o = 0.99$, $\alpha_u = p_u = 0.01$, $\sigma = 0.2$, and $\gamma = 0.2$. The value of β_E is set as follows: (a) $\beta_E = 0.2\beta_I$, (b) $\beta_E = 0.4\beta_I$, and (c) $\beta_E = 0.8\beta_I$.
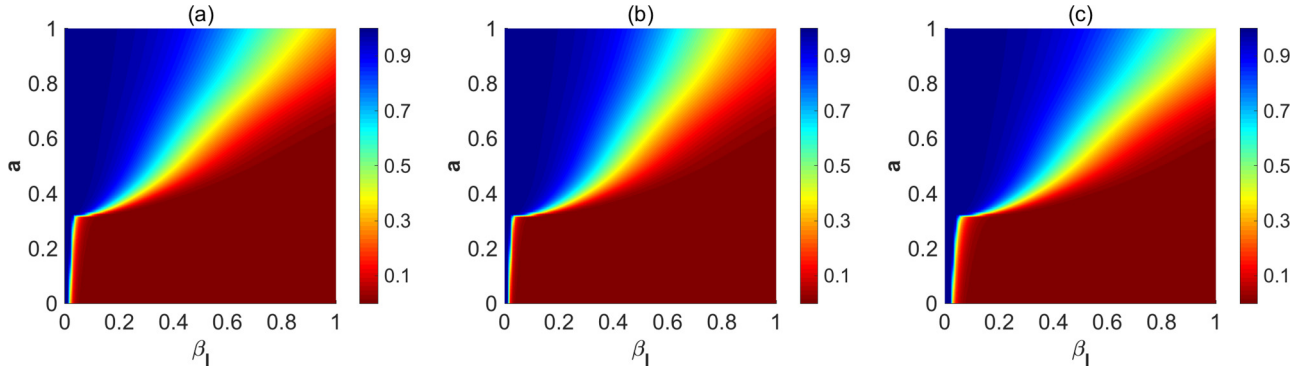
FIG. 6. Full a-β_I phase diagrams of the fraction of susceptible nodes at the stationary state $\rho_S(\infty)$ for different values of σ and γ with asymptomatically infected cases, where $\beta_E = 0.5\beta_I$, $\eta = 0.1$, $\alpha_o = p_o = 0.99$, and $\alpha_u = p_u = 0.01$. The values of σ and γ are set as follows: (a) $\sigma = 0.8$ and $\gamma = 0.2$, (b) $\sigma = 0.2$ and $\gamma = 0.2$, and (c) $\sigma = 0.2$ and $\gamma = 0.8$.

threshold, further highlighting this fraction is not necessary. This finding shows that the disease outbreak is preventable when the media and opinion leaders are playing effective roles of the whistleblower.

More specifically, when β_I is extremely small, all possible values of a yield the fully prevented scenario (blue). As β_I increases, the range of a rapidly increases and yields the full outbreak scenario (red). When β_I keeps increasing, the range of a yielding a full outbreak scenario gradually increases. We define the critical value of β_I as the value leading to the basic reproduction number $R_0 = \beta_I/\gamma = 1$, below which the epidemic is under control. As shown in Fig. 7(a), where a is fixed, the higher the recovery rate γ, the larger the critical value of β_I. Given the same β_I, we can observe an increase in $\rho_S(\infty)$ with a longer incubation period $1/\sigma$ or a smaller R_0 (larger γ) [see Fig. 7(a)]. It might be because a longer incubation period can provide more time for the awareness to be transmitted among people and a smaller R_0 means a less transmissible disease. Thus, a smaller fraction of overreacting nodes is needed to prevent the full outbreak.

Second, we consider the diseases with asymptomatically infected cases. Given that not all exposed individuals are asymptomatically infected and the asymptomatically infected

cases are often not more infectious than symptomatically infected cases [48–50,58], we define the asymptomatic infection rate as $\beta_E = \mu\beta_I$, where $\mu \in (0, 1)$. We report the fraction of susceptible nodes at the stationary state $\rho_S(\infty)$ in Fig. 5 where $\mu \in \{0.2, 0.4, 0.8\}$. The values of other parameters are the same as those in Fig. 4(b), where the asymptomatic infection is not considered. We find that when asymptomatic infections exist, the range of a yielding the full outbreak scenario is larger and the effect becomes more significant with a larger value of μ. In the extreme case when $\mu \to 1$, the disease transmission layer essentially becomes an SIR model with longer infectious period than the original SEIR model. These results indicate that asymptomatic infections make it harder, sometimes even impossible, to control the epidemic by only increasing the value of a [Fig. 5(c)].

Furthermore, we explore the effects of overreacting nodes with various parameter settings on the disease transmission layer (representing different diseases) in Fig. 6. Compared with the cases where $\beta_E = 0$, the existence of asymptomatic infections reduces the critical values of β_I and the values of $\rho_S(\infty)$, indicating that epidemic control is more difficult (see Fig. 7). With the existence of asymptomatically infected cases, $R_0 = \beta_I/\gamma + \beta_E/\sigma$ [59]. We find that not only the
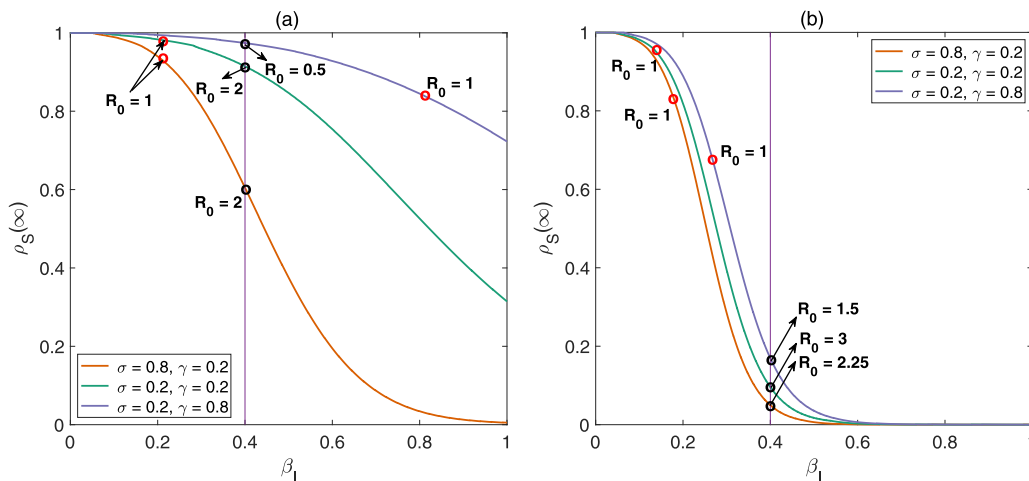

FIG. 7. Fraction of susceptible nodes at the stationary state $\rho_S(\infty)$ with respect to β_I for different values of σ and γ, where $a = 0.4$, $\eta = 0.1$, $\alpha_o = p_o = 0.99$, and $\alpha_u = p_u = 0.01$. The value of β_E is set as follows: (a) $\beta_E = 0$ and (b) $\beta_E = 0.5\beta_I$.
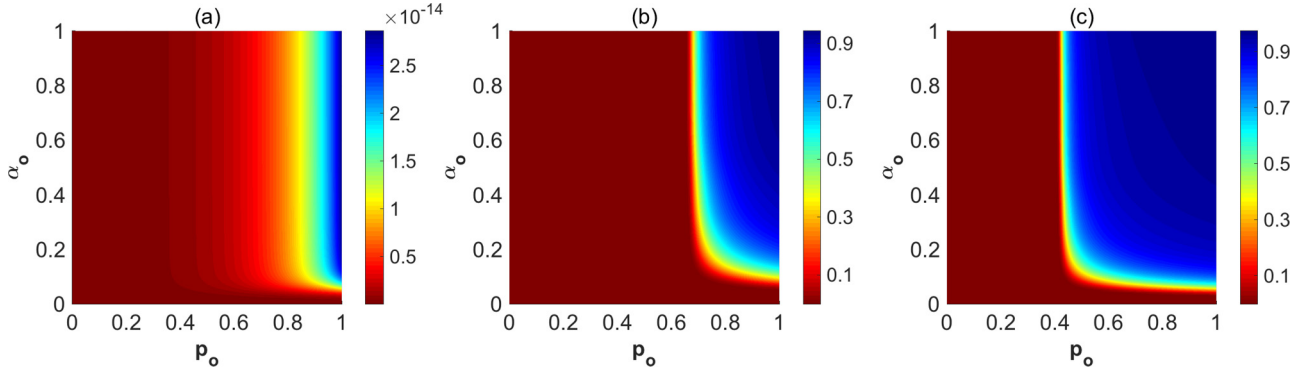
FIG. 8. Full α_o-p_o phase diagrams of the fraction of susceptible nodes at the stationary state $\rho_S(\infty)$ for different values of a, where $\beta_I = 0.5$, $\beta_E = 0$, $\sigma = \gamma = 0.2$, and $\eta = 0.1$. The value of a is set as follows: (a) $a = 0.1$, (b) $a = 0.5$, and (c) $a = 0.8$.

higher recovery rate γ but also the shorter incubation period $1/\sigma$ can increase the critical value of β_I. A smaller R_0 does not always lead to a larger $\rho_S(\infty)$ in such cases. As illustrated in Fig. 7(b), given the same β_I, when γ increases to 0.8 from 0.2, R_0 drops to 1.5 from 3. Thus, $\rho_S(\infty)$ increases for a less transmissible disease. However, when σ increases to 0.8 (shorter incubation period), R_0 decreases to 2.25 from 3 (less transmissible). Counterintuitively, $\rho_S(\infty)$ decreases to 0.05 from 0.096. That is because a larger σ not only leads to a smaller R_0 but also indicates a shorter incubation time for the awareness to spread out; therefore, fewer people are aware and protected.

Third, we further clarify the effect of overreacting nodes on epidemic control for different values of α and p in Fig. 8 (for grayscale versions of Figs. 4–6 and 8, see the Supplemental Material [60]). For simplicity, we assume $\alpha_u = \frac{1}{2}\alpha_o$ and $p_u = \frac{1}{2}p_o$. Fewer nodes will be infected when α and p increase. When the value of a increases, the epidemic is easier to control (a larger blue region in the figure). A small transitioning space occurs between controlled (blue) and outbreak (red) scenarios, indicating that the epidemic either can be well contained or will likely infect the majority of people in the population.

Finally, we examine the fraction of susceptible nodes at the stationary state $\rho_S(\infty)$ in two scenarios: with and without social influence on behavior change. Here the scenario without social influence is modeled by setting $W = 0$ regardless of the behavior of the node's neighbors. We consider two diseases with different parameter settings in Fig. 9. With the social influence on behavior change, we can achieve the fully controlled result $[\rho_S(\infty) \to 1]$ with a lower value of a for both diseases, indicating that we can effectively utilize the social influence among people to enhance the disease prevention.

To further clarify such a significant effect on $\rho_S(\infty)$, we focus on one specific disease setting mentioned in Fig. 9 and analyze the fraction of nodes in states S and A $[\rho_S(t)$ and $\rho_A(t)]$ and the probability of changing behavior due to the social influence from neighbors (W) over time in Fig. 10. Here we consider two scenarios, where $a = 0.2$ and 0.4, respectively. We observe that W increases rapidly over time and reaches an equilibrium state for both cases. Larger a leads to a higher value of W at the equilibrium state. Assuming that the information diffusion layer reaches the equilibrium state at time t_I and W reaches the equilibrium state at time t_W and

setting $T = \max\{t_I, t_W\}$, we obtain

$$
\begin{aligned}
\rho_A(T) &= [\rho_{SP}(T) + \rho_{SF}(T)]\{ap_o + (1-a)p_u \\
&\quad + [a(1-p_o) + (1-a)(1-p_u)]W\} \\
&= [\rho_{SP}(T) + \rho_{SF}(T)][ap_o + (1-a)p_u] \\
&\quad + [\rho_{SP}(T) + \rho_{SF}(T)][a(1-p_o) \\
&\quad + (1-a)(1-p_u)]W
\end{aligned}
\tag{12}
$$

from Eq. (6), indicating that the fraction of people who have adopted self-protection, $\rho_A(T)$, can be increased with the help of social influence. In addition,

$$
\rho_{IG}(T) = \rho_{IG}(T)[1 - h(T)],
\tag{13}
$$

which indicates that $\rho_{IG}(T) = 0$ or $h(T) = 0$; $h(T) = 0$ only if $\rho_{SP}(T) = 0$ according to Eq. (5). We can derive that if $\bar{k}[a\alpha_o + (1-a)\alpha_u] > 1$, where $\bar{k}$ is the mean degree of the network, then information can always spread out $[\rho_{SP}(T) > 0]$ [41]. In such cases, $h(T) \neq 0$, and thus $\rho_{IG}(T) = 0$, indicating that $\rho_{SP}(T) + \rho_{SF}(T) = 1$. Therefore, Eq. (12) can be simplified as

$$
\rho_A(T) = ap_o + (1-a)p_u + [a(1-p_o) + (1-a)(1-p_u)]W
\tag{14}
$$

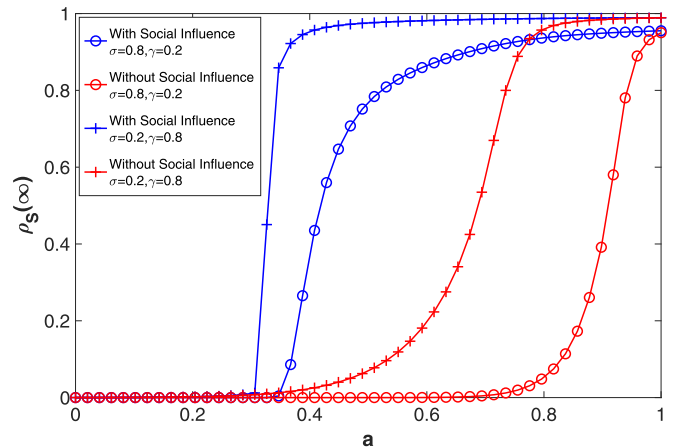if $\bar{k}[a\alpha_o + (1-a)\alpha_u] > 1$.

FIG. 9. Comparison of the fraction of susceptible nodes at the stationary state $\rho_S(\infty)$ with respect to a for two diseases, where $\eta = 0.1$, $\alpha_o = p_o = 0.99$, $\alpha_u = p_u = 0.01$, $\beta_I = 0.5$, and $\beta_E = 0$.
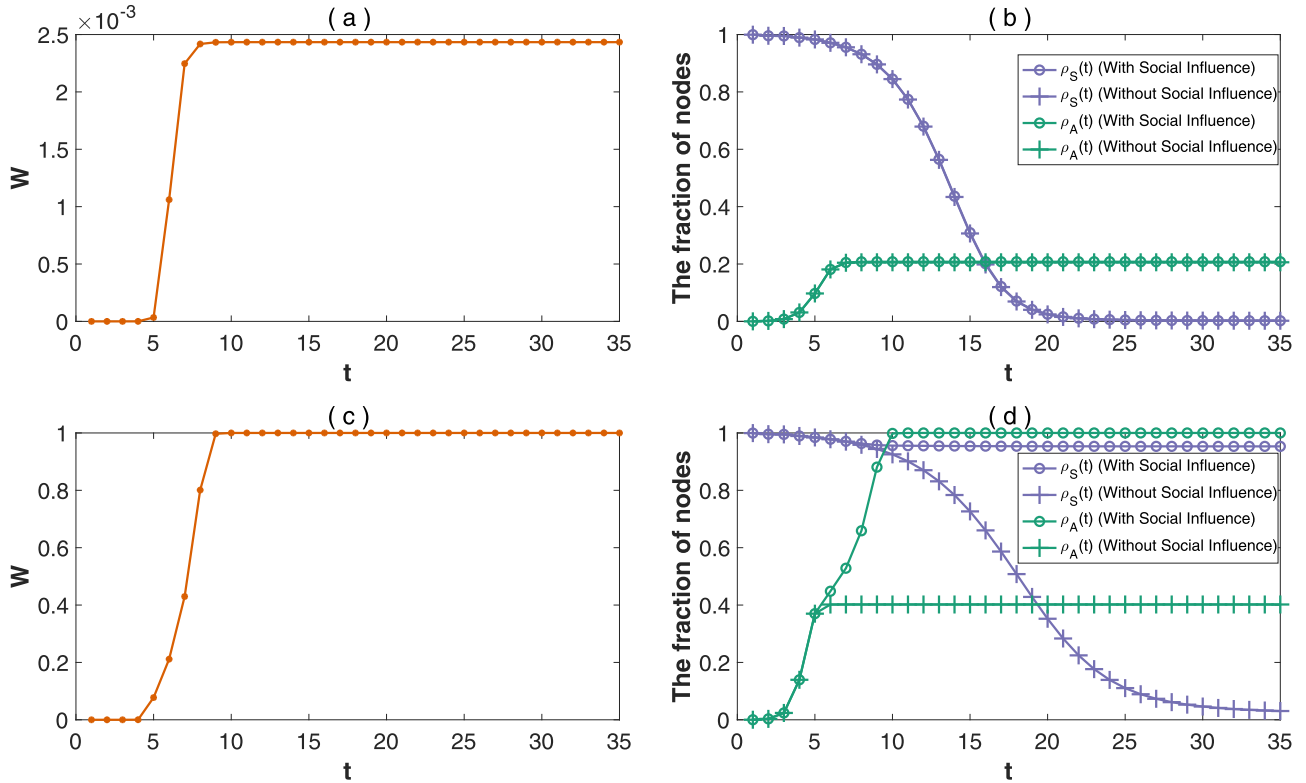
FIG. 10. Effect of social influence on the epidemic with different fractions of overreacting nodes. (a) and (c) Probability of changing behavior due to the social influence from neighbors (W) at time t. (b) and (d) Fraction of susceptible nodes $\rho_S(t)$ and fraction of nodes having adopted self-protection $\rho_A(t)$ over time, with (a) and (b) $a = 0.2$ and (c) and (d) $a = 0.4$. The other parameters are $\beta_I = 0.5$, $\beta_E = 0$, $\sigma = 0.2$, $\gamma = 0.8$, $\eta = 0.1$, $\alpha_o = p_o = 0.99$, and $\alpha_u = p_u = 0.01$.

When $a = 0.2$, the value of W at $t = T$ is small, indicating that social influence has little effect on the behavior change. In such cases, $\bar{k}[a\alpha_o + (1-a)\alpha_u] = 3.09 > 1$ and then $\rho_A(T) \approx a p_o + (1-a)p_u = 0.206$, which is small, indicating that the epidemic cannot be well contained. However, when $a = 0.4$, W reaches 1 rapidly and $\bar{k}[a\alpha_o + (1-a)\alpha_u] = 6.03 > 1$; then $\rho_A(T) = 1$. Thus, the actual infection rate $l(\beta) = \beta\eta^2$ is close to 0 for small η according to Eq. (8). As a result, the transition probability for a susceptible node being infected is $c(T) \to 0$ according to Eq. (9), indicating that the epidemic is approaching the end. Since $\rho_S(t)$ is decreasing over time, the earlier $c(t)$ becomes 0, the fewer people are infected. Therefore, the fraction of susceptible nodes tends to remain high since $t = T$ with the existence of social influence, which happens earlier than without social influence [Fig. 10(d)]. These results indicate that social influence on behavior change can significantly accelerate behavior change and lead to a smaller epidemic outbreak.

V. CONCLUSION

In this study we have developed a heterogeneous disease-behavior-information transmission model to characterize the heterogeneous processes of information diffusion, behavior change, and disease transmission on social networks. We adopted the mean-field approximation approach to obtain analytical results and perform extensive Monte Carlo simulations

to examine the patterns of disease transmission in the presence of information diffusion and behavior change among people. We found that (a) disease awareness plays a central role in preventing the disease outbreak, (b) a reasonable fraction of overreacting nodes is needed to effectively control the epidemic, and (c) a smaller basic reproduction number R_0 always leads to a smaller epidemic outbreak without symptomatically infected cases. This scenario would have different effects with asymptomatically infected cases because a smaller R_0 might result from a shorter incubation time. As a result, people have a shorter period to become aware and adopt self-protection. We also found that (d) social influence on behavior change can significantly decrease the outbreak size.

In practice, in the absence of vaccines and stringent control measures, the epidemic can still be well contained when people are aware of the disease and adopt proper self-protection. The media and opinion leaders play a key role in people's disease awareness. If transmissibility and severity are understated by them, then more people will remain underreacting and thus will be infected eventually. However, if they state unreasonably high transmissibility and severity of the disease, the "crying wolf" effect could result in people losing confidence in the public health system. Further research is needed to identify the optimal degree of transmissibility and severity stated by the media and opinion leaders. This research has limitations. In the current model, we assume an unchanged topological structure of the multiplex network, but uninfected

nodes might break connections with infected nodes and form new connections with other uninfected nodes to avoid being infected during epidemics. Incorporating the adaptive network schemes into the current model by introducing a rewiring probability for uninfected nodes is left for future work. In the COVID-19 context, many countries have seen protests against the lockdown measures, indicating that stiflers could even become another type of competing spreaders that influence ignorants to become stiflers. Modeling the competing behaviors during epidemics is an interesting topic for further exploration.

[1] WHO, Protect yourself and others, http://www.emro.who.int/health-topics/corona-virus/protect-yourself-and-others.html (WHO, Cairo, 2020).

[2] N. Ferguson, Nature (London) **446**, 733 (2007).

[3] G. J. Rubin, R. Amlôt, L. Page, and S. Wessely, BMJ **339**, b2651 (2009).

[4] J. T. F. Lau, X. Yang, H. Tsui, and J. H. Kim, J. Epidemiol. Commun. Health **57**, 864 (2003).

[5] T. Philipson, J. Hum. Resour. **31**, 611 (1996).

[6] K. Macintyre, L. Brown, and S. Sosler, AIDS Educ. Prev. **13**, 160 (2001).

[7] S. Collinson and J. M. Heffernan, BMC Public Health **14**, 376 (2014).

[8] J. J. Van Bavel, K. Baicker, P. S. Boggio, V. Capraro, A. Cichocka, M. Cikara, M. J. Crockett, A. J. Crum, K. M. Douglas, J. N. Druckman *et al.*, Nat. Hum. Behav. **4**, 460 (2020).

[9] L. Li, Q. Zhang, X. Wang, J. Zhang, T. Wang, T. Gao, W. Duan, K. K. Tsoi, and F. Wang, IEEE Trans. Comput. Soc. Syst. **7**, 556 (2020).

[10] N. Perra, B. Gonçalves, R. Pastor-Satorras, and A. Vespignani, Sci. Rep. **2**, 469 (2012).

[11] Z. Wang, H. Zhang, and Z. Wang, Chaos Soliton. Fractal. **61**, 1 (2014).

[12] S. Ruan and W. Wang, J. Differ. Equations **188**, 135 (2003).

[13] Z. Wang, M. A. Andrews, Z.-X. Wu, L. Wang, and C. T. Bauch, Phys. Life Rev. **15**, 1 (2015).

[14] K. A. Kabir, K. Kuga, and J. Tanimoto, Chaos Soliton. Fractal. **132**, 109548 (2020).

[15] D. Han, Q. Shao, D. Li, and M. Sun, Appl. Math. Comput. **369**, 124894 (2020).

[16] D. Guo, S. Trajanovski, R. van de Bovenkamp, H. Wang, and P. Van Mieghem, Phys. Rev. E **88**, 042802 (2013).

[17] E. P. Fenichel, C. Castillo-Chavez, M. G. Ceddia, G. Chowell, P. A. G. Parra, G. J. Hickling, G. Holloway, R. Horan, B. Morin, C. Perrings *et al.*, Proc. Natl. Acad. Sci. USA **108**, 6306 (2011).

[18] S. Collinson, K. Khan, and J. Heffernan, PLoS One **10**, e0141423 (2015).

[19] S. Funk, E. Gilad, C. Watkins, and V. A. Jansen, Proc. Natl. Acad. Sci. USA **106**, 6872 (2009).

[20] T. Gross, C. J. D. D'Lima, and B. Blasius, Phys. Rev. Lett. **96**, 208701 (2006).

[21] Q. Wu, X. Fu, M. Small, and X.-J. Xu, Chaos **22**, 013101 (2012).

[22] F. H. Chen, Math. Biosci. **217**, 125 (2009).

[23] M. Kurant and P. Thiran, Phys. Rev. Lett. **96**, 138701 (2006).

[24] M. Kivelä, A. Arenas, M. Barthelemy, J. P. Gleeson, Y. Moreno, and M. A. Porter, J. Complex Netw. **2**, 203 (2014).

[25] C. Granell, S. Gómez, and A. Arenas, Phys. Rev. Lett. **111**, 128701 (2013).

[26] Y. Pan and Z. Yan, Physica A **491**, 45 (2018).

[27] Q. Guo, X. Jiang, Y. Lei, M. Li, Y. Ma, and Z. Zheng, Phys. Rev. E **91**, 012822 (2015).

[28] K. A. Kabir, K. Kuga, and J. Tanimoto, Chaos Soliton. Fractal. **119**, 118 (2019).

[29] L. Mao, Appl. Geogr. **50**, 31 (2014).

[30] C. Granell, S. Gómez, and A. Arenas, Phys. Rev. E **90**, 012808 (2014).

[31] N. Perra, D. Balcan, B. Gonçalves, and A. Vespignani, PLoS ONE **6**, e23084 (2011).

[32] R. Liu, J. Wu, and H. Zhu, Comput. Math. Methods Med. **8**, 153 (2007).

[33] A. Wang and Y. Xiao, Nonlinear Anal.: Hybrid Syst. **11**, 84 (2014).

[34] P. Dubey, B. Dubey, and U. Dubey, in *BIOMAT 2015 : Proceedings of the International Symposium on Mathematical and Computational Biology, Roorkee, 2015*, edited by R. P. Mondaini (World Scientific, Singapore, 2015).

[35] E. M. Cramer, H. Song, and A. M. Drent, Comput. Hum. Behav. **64**, 739 (2016).

[36] P. Song and Y. Xiao, J. Math. Biol. **76**, 1249 (2018).

[37] P. Song and Y. Xiao, Bull. Math. Biol. **81**, 1582 (2019).

[38] L. Sjôberg, Risk Anal. **20**, 1 (2000).

[39] A. A. Wahlberg and L. Sjoberg, J. Risk Res. **3**, 31 (2000).

[40] R. S. B. Renner, M. Gamp, and H. T. Schupp, in *International Encyclopedia of the Social and Behavioral Sciences*, 2nd ed., edited by J. D. Wright (Elsevier, Oxford, 2015), pp. 702–709.

[41] Z. Ruan, J. Wang, Q. Xuan, C. Fu, and G. Chen, Phys. Rev. E **98**, 022308 (2018).

[42] Z. Ruan, M. Tang, and Z. Liu, Phys. Rev. E **86**, 036117 (2012).

[43] N. Zhu, D. Zhang, W. Wang, X. Li, B. Yang, J. Song, X. Zhao, B. Huang, W. Shi, R. Lu *et al.*, New Engl. J. Med. **382**, 727 (2020).

[44] C. Wang, P. W. Horby, F. G. Hayden, and G. F. Gao, Lancet **395**, 470 (2020).

[45] G. J. Asmundson and S. Taylor, J. Anxiety Disord. **70**, 102196 (2020).

[46] D. Kai, G.-P. Goldstein, A. Morgunov, V. Nangalia, and A. Rotkirch, arXiv:2004.13553.

[47] F. D. Sahneh, C. Scoglio, and P. Van Mieghem, IEEE/ACM Trans. Netw. **21**, 1609 (2013).

[48] A. Wilder-Smith, M. D. Teleman, B. H. Heng, A. Earnest, A. E. Ling, and Y. S. Leo, Emerg. Infect. Dis. **11**, 1142 (2005).

[49] C. Rothe, M. Schunk, P. Sothmann, G. Bretzel, G. Froeschl, C. Wallrauch, T. Zimmer, V. Thiel, C. Janke, W. Guggemos, M. Seilmaier, C. Drosten, P. Vollmar, K. Zwirglmaier, S. Zange, R. Wölfel, and M. Hoelscher, New Engl. J. Med. **382**, 970 (2020).

[50] J. Papenburg, M. Baz, M.-È. Hamelin, C. Rhéaume, J. Carbonneau, M. Ouakki, I. Rouleau, I. Hardy, D. Skowronski, M. Roger *et al.*, Clin. Infect. Dis. **51**, 1033 (2010).

[51] C. Hou, J. Chen, Y. Zhou, L. Hua, J. Yuan, S. He, Y. Guo, S. Zhang, Q. Jia, C. Zhao *et al.*, J. Med. Virol. **92**, 841 (2020), special issue on new coronavirus (2019-nCoV or SARS-CoV-2) and the outbreak of the respiratory illness (COVID-19): Part-IV, edited by G. Luo and S.-J. Gao.

[52] J. T. Wu, K. Leung, and G. M. Leung, Lancet **395**, 689 (2020).

[53] A.-L. Barabási, R. Albert, and H. Jeong, Physica A **272**, 173 (1999).

[54] C. Li, R. van de Bovenkamp, and P. Van Mieghem, Phys. Rev. E **86**, 026116 (2012).

[55] P. G. Fennell, S. Melnik, and J. P. Gleeson, Phys. Rev. E **94**, 052125 (2016).

[56] L. J. Allen and A. M. Burgin, Math. Biosci. **163**, 1 (2000).

[57] H. W. Hethcote, SIAM Rev. **42**, 599 (2000).

[58] S. Lee, T. Kim, E. Lee, C. Lee, H. Kim, H. Rhee, S. Y. Park, H.-J. Son, S. Yu, J. W. Park *et al.*, JAMA Intern. Med. (2020), doi:10.1001/jamainternmed.2020.3862.

[59] G. Oliveira, arXiv:2004.14780.

[60] See Supplemental Material at http://link.aps.org/supplemental/10.1103/PhysRevE.102.042314 for grayscale versions of Figs. 4–6 and 8.